Check for updates

RESEARCH ARTICLE

REVISED Manipulating and measuring single atoms in the Maltese cross geometry

[version 2; peer review: 2 approved]

Lorena C. Bianchet[1], Natalia Alves[1], Laura Zarraoa[1], Natalia Bruno[2,3], Morgan W. Mitchell[1,4]

[1]ICFO - Institut de Ciències Fotòniques, The Barcelona Institute of Science and Technology, Castelldefels, Barcelona, 08860, Spain
[2]Istituto Nazionale di Ottica (CNR-INO), Largo Enrico Fermi 6, Florence, 50125, Italy
[3]European Laboratory for Non-linear Spectroscopy (LENS), Via nello Carrara 1, 50019 Sesto Fiorentino, Florence, Italy
[4]ICREA - Institució Catalana de Recerca i Estudis Avançats, Barcelona, 08010, Spain

v2 **First published:** 06 Sep 2021, **1**:102
https://doi.org/10.12688/openreseurope.13972.1
Latest published: 03 Mar 2022, **1**:102
https://doi.org/10.12688/openreseurope.13972.2

Abstract

Background: Optical microtraps at the focus of high numerical aperture (high-NA) imaging systems enable efficient collection, trapping, detection and manipulation of individual neutral atoms for quantum technology and studies of optical physics associated with super- and sub-radiant states. The recently developed "Maltese cross" geometry (MCG) atom trap uses four in-vacuum lenses to achieve four-directional high-NA optical coupling to single trapped atoms and small atomic arrays. This article presents the first extensive characterisation of atomic behaviour in a MCG atom trap.
Methods: We employ a MCG system optimised for high coupling efficiency and characterise the resulting properties of the trap and trapped atoms. Using current best practices, we measure occupancy, loading rate, lifetime, temperature, fluorescence anti-bunching and trap frequencies. We also use the four-directional access to implement a new method to map the spatial distribution of collection efficiency from high-NA optics: we use the two on-trap-axis lenses to produce a 1D optical lattice, the sites of which are stochastically filled and emptied by the trap loading process. The two off-trap-axis lenses are used for imaging and single-mode collection. Correlations of single-mode and imaging fluorescence signals are then used to map the single-mode collection efficiency.
Results: We observe trap characteristics comparable to what has been reported for single-atom traps with one- or two-lens optical systems. The collection efficiency distribution in the axial and transverse directions is directly observed to be in agreement with expected collection efficiency distribution from Gaussian beam optics.
Conclusions: The multi-directional high-NA access provided by the Maltese cross geometry enables complex manipulations and measurements not possible in geometries with fewer directions of access, and can be achieved while preserving other trap

Open Peer Review

Approval Status ✓ ✓

	1	2
version 2 (revision) 03 Mar 2022		
version 1 06 Sep 2021	✓ view	✓ view

1. **Daniel Barredo**, Université Paris-Saclay, Palaiseau, France

2. **Chi Huan Nguyen**, National University of Singapore, Singapore, Singapore
Chang Hoong Chow, Centre for Quantum Technologies, Singapore, Singapore

Any reports and responses or comments on the article can be found at the end of the article.

characteristics such as lifetime, temperature, and trap size.

Keywords
Single atom, high numerical aperture, optical tweezers, Maltese cross, optical lattice, resonance fluorescence, single quantum emitter, parametric excitation



This article is included in the Horizon 2020 gateway.



This article is included in the Optics gateway.

Corresponding authors: Lorena C. Bianchet (lorena.bianchet@icfo.eu), Morgan W. Mitchell (morgan.mitchell@icfo.eu)

Author roles: Bianchet LC: Conceptualization, Data Curation, Formal Analysis, Investigation, Methodology, Software, Validation, Visualization, Writing – Original Draft Preparation, Writing – Review & Editing; **Alves N**: Conceptualization, Data Curation, Formal Analysis, Investigation, Methodology, Software, Validation, Visualization, Writing – Original Draft Preparation, Writing – Review & Editing; **Zarraoa L**: Investigation, Writing – Review & Editing; **Bruno N**: Conceptualization, Investigation, Writing – Review & Editing; **Mitchell MW** : Conceptualization, Formal Analysis, Funding Acquisition, Methodology, Project Administration, Supervision, Visualization, Writing – Original Draft Preparation, Writing – Review & Editing

Competing interests: No competing interests were disclosed.

Grant information: This research was financially supported by the European Union's Horizon 2020 research and innovation programme under the grant agreement No [820405](Quantum Random Number Generators [QRANGE]). This work was also supported by La Caixa Foundation (Fundación Bancaria Caixa d'Estalvis i Pensions de Barcelona) under agreement [LCF/BQ/SO15/52260044]; Severo Ochoa Center of Excellence, Generalitat de Catalonia, through the Centres de Recerca de Catalunya (CERCA) program [CEX2019-000910-S]; Spanish Ministry of Science and Innovation (Ministerio de Ciencia e Innovación) projects OCARINA [PGC2018-097056-B-I00] and Q-CLOCKS [PCI2018-092973]; Agency for Management of University and Research Grants (Agència de Gestió d'Ajuts Universitaris i de Recerca)[2017-SGR-1354]; Department of Research and Universities of the Department of Business and Employment of the Generalitat de Catalunya (Secretaria d'Universitats i Recerca del Departament d'Empresa i Coneixement de la Generalitat de Catalunya), co-funded by the European Union Regional Development Fund within the ERDF Operational Program of Catalunya, project QuantumCat [001-P-001644], as well as the European Social Fund (L'FSE inverteix en el teu futur) - FEDER; CELLEX Foundation (Fundació Privada Cellex); Fundació Mir-Puig; the European Metrology Programme for Innovation and Research (EMPIR) programme [17FUN03-USOQS] co-financed by the Participating States and from the European Union's Horizon 2020 research and innovation programme.
The funders had no role in study design, data collection and analysis, decision to publish, or preparation of the manuscript.

Copyright: © 2022 Bianchet LC *et al*. This is an open access article distributed under the terms of the Creative Commons Attribution License, which permits unrestricted use, distribution, and reproduction in any medium, provided the original work is properly cited.

How to cite this article: Bianchet LC, Alves N, Zarraoa L *et al.* **Manipulating and measuring single atoms in the Maltese cross geometry [version 2; peer review: 2 approved]** Open Research Europe 2022, **1**:102 https://doi.org/10.12688/openreseurope.13972.2

First published: 06 Sep 2021, **1**:102 https://doi.org/10.12688/openreseurope.13972.1

REVISED **Amendments from Version 1**

This version of the article includes additional details of some of the experimental procedures, as requested by the reviewers. The section "Occupancy and loading rate" has been expanded. Additionally, some small errors in the main text have been corrected.

Any further responses from the reviewers can be found at the end of the article

Plain language summary

In this article we report measurements performed on individual atoms held in place by focused laser beams. The atoms are in vacuum, which prevents them from coming into contact with other atoms or molecules. By using four lenses, placed around the equator of a sphere centered on the atom, we are able to collect light emitted by the atom in different directions, and also to illuminate the atom from different directions simultaneously. One of the main aims of this work is to measure the characteristics of an atom trapped in this kind of four-lens system. We measure the rate at which atoms are collected into the trap, how long they remain before leaving, the average kinetic energy of the atom, the emission pattern that evidences the presence of the atom in the trap and a measure of the time correlations of the emitted photons. The results show that in the system with four lenses, the atom is as cold and well-localized as in one- and two-lens systems previously characterized. To demonstrate the possibilities created by having lenses along four directions, we send laser light at the atom from two opposing directions, while also collecting light emitted from the atom along three directions. By sending light along two opposing directions, we create many small traps at which the atom can be immobilized. This allows us to study how well the lenses can collect light from different locations, and in particular demonstrates the ability to selectively collect light from some locations rather than others.

Introduction

Optical microtraps at the focus of high numerical aperture (high-NA) imaging systems enable efficient collection, trapping, detection and manipulation of individual neutral atoms[1–5] and molecules[6]. These capabilities are exploited in several active topics in quantum optics and quantum technology, including strong single-atom effects on traveling-wave beams[7–12], higher-order interference of atoms[13–15] and Rydberg-atom-based quantum information processing[16] and quantum simulation[17,18]. High-NA trapping systems may also enable strong modifications to radiation physics associated with sub-radiant states[19–22].

The earliest experiments with neutral-atom microtraps employed large vacuum systems and custom-designed optics[23]. More recent works have employed high-NA aspheric lenses[24] in smaller vacuum systems, which has enabled experiments with high-NA optical access from two[8,25] and four[26–29] directions. The four-lens arrangement is known as the Maltese cross geometry (MCG) when the lenses are placed on the cardinal directions, as illustrated in Figure 1.

The MCG can increase the total solid angle coupled to the atom[28], and makes possible the measurement of coherent, large-momentum-transfer scattering processes in disordered ensembles[30] and in atomic arrays[19], for which strong sub-radiant effects are predicted. The right-angle geometry is also predicted to enhance and modify the observable quantum correlations in resonance fluorescence[31]. The MCG geometry also imposes constraints not present in traps using one or two lenses. Most immediately, the direct (as opposed to through-lens) optical access is greatly reduced in the plane of the four lenses. Forming a magneto-optical trap (MOT) then either requires reduced NA[32], a non-orthogonal beam geometry[8] or a sub-mm

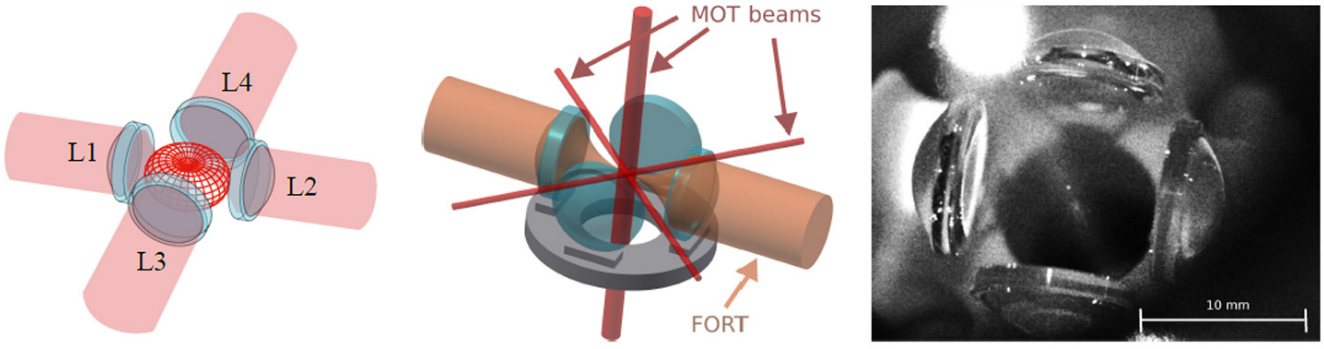


Figure 1. Illustration of the Maltese cross geometry, in which four high-numerical-aperture lenses L1 to L4 are arranged along the cardinal axes. Left: Red meshed structure at center shows the angular distribution of radiation from a vertically-polarized electric dipole transition. The emission is strongest around the equator and thus efficiently collected by the four lenses. Center: In addition to collecting light efficiently, the in-vacuum aspheric lenses can be used for strongly-focused illumination, and to efficiently produce a far-off-resonance trap (FORT). The in-vacuum lenses leave little open solid angle in the equator for magneto-optical trap (MOT) beams, which are necessarily much smaller than in a typical MOT. Right: image of the four-lens assembly used in this work. The small bright spot at the centre of the lens arrangement is the MOT. Large bright spot at the upper left is scattering of the vertically-propagating MOT beams from the vacuum chamber window.

beam diameter[26]. In the system described here, we use four in-vacuum high-NA aspheric lenses, and pass sub-mm MOT beams through the small gaps between them, as shown in Figure 2. This approach leads to greatly reduced MOT volume and atom number[28]. At the same time, the use of simple aspheric lenses, rather than multi-element objectives, implies a small diffraction-limited focal region of ~ 30 μm diameter, and also different focal lengths for the 780 nm fluorescence wavelength versus the 852 nm far-off-resonance trap (FORT) wavelength[28]. While physical-optics simulations in Zemax, described in 28, indicate that it should still be possible to achieve diffraction-limited spot sizes for four fluorescence-coupling beams and the FORT beams producing the trap, the tolerances are reduced relative to lens geometries that only couple from one or two directions. These potential perturbations to the cooling and trapping components of the system motivate a characterization of the MCG system's capacity to produce and optically couple to cold, well-localized trapped atoms and atomic arrays.

In this article we check that the incorporation of a third and fourth lens has not degraded the optical system's ability to trap, cool and couple light to single atoms. To this end, we measure occupancy, loading rate, lifetime, temperature, fluorescence anti-bunching and trap frequencies using current best practices.

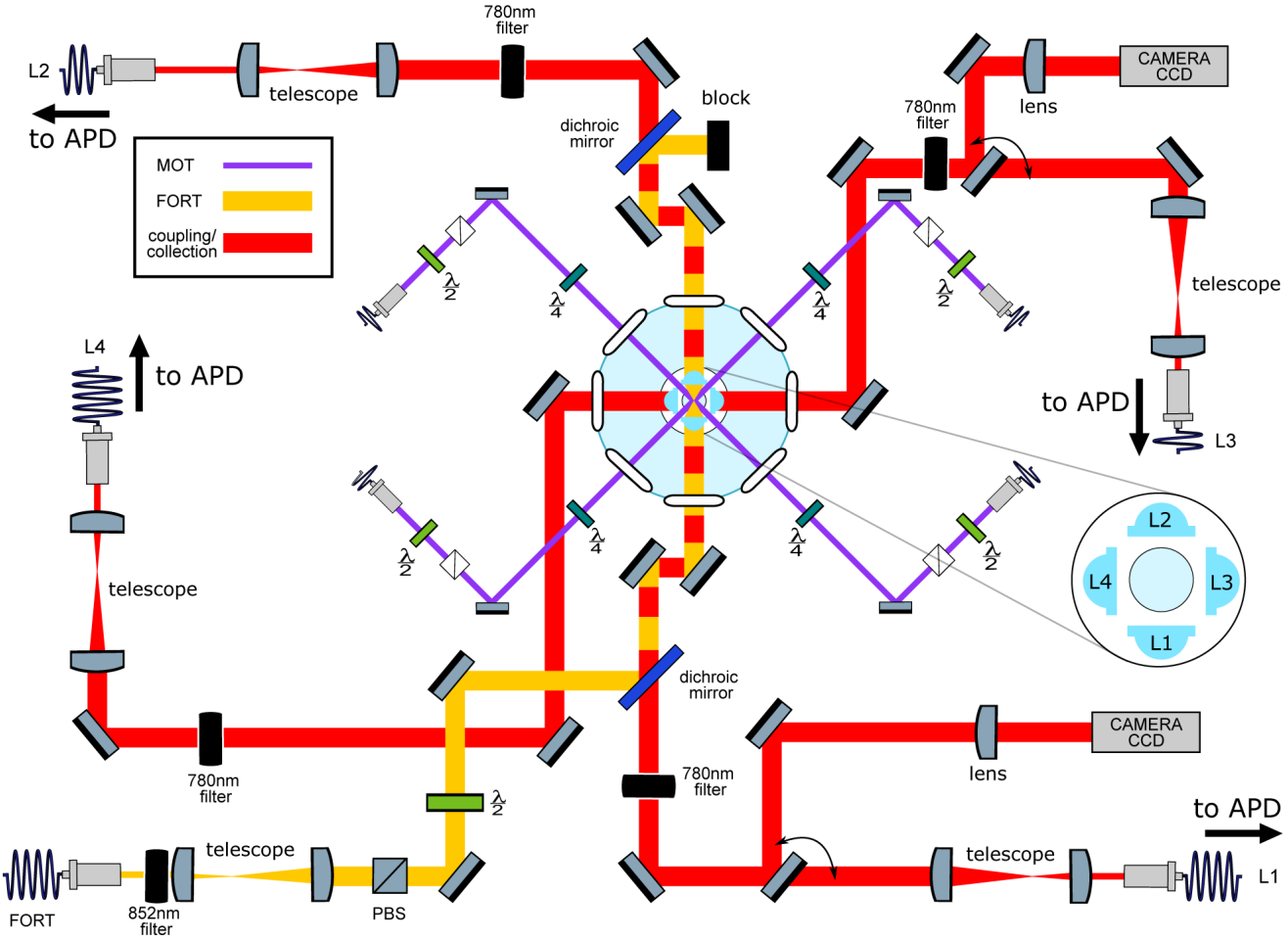


Figure 2. Main elements of the optical setup. Left: Schematic of optical systems. Nearly all elements lie in a horizontal plane intersecting the trap center. In light blue: Four aspheric lenses (lens numbers L1-L4 are indicated in the inset) are located symmetrically around the geometric center of a "spherical octagon" vacuum enclosure with eight anti-reflection-coated windows. In purple: magneto-optical trap (MOT) beams, which pass through the gaps between the lenses; vertically-directed MOT beams passing through the trap center are not shown. In yellow: far-off-resonance trap (FORT) beam, which is focused by L1 and re-collimated by L2. The beam-block shown in the image can be replaced with a mirror to retro-reflect the beam and produce a 1D lattice, as described in section **Collection-efficiency mapping using stochastic loading**. In red: Beams focused by the in-vacuum lenses for coupling light to and from the single atom. Red/yellow dashing: Coupling beams leading to L1 and L2 are combined on dichroic mirrors with the FORT beam, resulting in coaxial propagation. All four lenses can be used for fluorescence collection, which is either collected with a fiber and sent to an avalanche photodiode detector (APD) or sent to a charge-coupled device (CCD) camera in the case of L1 and L3. Diagram symbols: PBS: polarizing beamsplitter, $\lambda/2$ ($\lambda/4$): half (quarter) waveplate, filter: bandpass filters centered in the specified wavelength.

To our knowledge, these characterizations have not been reported for any four-lens trapping system. We observe trap characteristics comparable to what has been reported for single-atom traps with one- or two-lens optical systems, thus confirming that the MCG provides significant advantages in flexibility and total degree of coupling, without sacrificing other desirable features. With this utilitarian objective completed, we explore the new geometry's capabilities and characterize its spatial collection. To do so, we employ each of the four lenses in a different way in a single experiment, to produce an optical lattice, perform single-mode light collection both on-axis and off-axis, and also collect off-axis light onto an imaging sensor. This allows us to observe the stochastic loading and unloading of an optical lattice with three distinct collection modalities, and to quantify spatio-temporal correlations among them. In this way we are able to map the spatial distribution of collection efficiency of both on-axis and off-axis single-mode collection.

The article is organized as follows: In section **System description** we describe the experimental system, including MOT, far-off-resonance trap (FORT), and atomic fluorescence collection. In section **Trap characterization** we characterize the trap lifetime, temperature, and trap frequencies. In section **Collection-efficiency mapping using stochastic loading**. we measure the spatial distribution of collection efficiency for one axial and one transverse high-NA collection lens, using the correlation of fluorescence seen in single-mode collection with that seen in imaging detection.

System description

The system employs a small MOT to collect and cool a cloud of rubidium-87 (^{87}Rb) atoms from background vapor in an ultra-high vacuum enclosure, and load them into a FORT located within the MOT volume. The MOT and FORT centers are co-located at the center of a system of four high-NA lenses (NA=0.5) along the cardinal axes. As viewed from the FORT, each lens collects a solid angle of $2\pi\left(1-\sqrt{1-\mathrm{NA}^2}\right) \approx 0.27\pi$. A detailed description of the high-NA optics, assembly and characterization is given in 28. Here we describe other critical elements of the trapping and cooling system, which is illustrated in Figure 2.

MOT

A small MOT is formed by six counter-propagating beams along three orthogonal axes in the standard configuration. Repumper light is on resonance with the D_2 transition $5S_{1/2}$, $F = 1 \rightarrow 5P_{3/2}$, $F' = 2$, where F (F') indicates the hyperfine level of the $5S_{1/2}$ ground state ($5P_{3/2}$ excited state). Cooler light is red-detuned from the $5S_{1/2}$, $F = 2 \rightarrow 5P_{3/2}$, $F' = 3$ transition by $6\Gamma_0$, where $\Gamma_0 = 2\pi \times 6.06$ MHz is the D_2 natural linewidth. To pass cleanly between the 1.2 mm gaps separating the lenses, the horizontally-directed beams are of 0.7mm diameter, whereas the vertical beams are of 2.0mm diameter[1]. Horizontal and vertical cooler beams have powers of 20 μW and 162 μW, respectively. Repump light of 150 μW is sent only in the downward vertical direction, to minimize scattered light. For the single-atom experiments described below, a MOT gradient of 3.8 G cm^{-1} is used, to reduce the number of MOT atoms and resulting background fluorescence. In this scenario, we produce a ≈ 50 μm diameter cloud of cold atoms to be superimposed with the FORT described in section **FORT**.

FORT

The FORT is produced by a linearly-polarized 852 nm beam with a power of 7 mW and a beam waist of 1.85 mm at the aspheric lens position. The laser used to produce this beam is a distributed feedback (DFB) laser (Toptica Eagleyard EYPDFB0852) stabilized to the $6S_{1/2}$, $F = 4 \rightarrow 6P_{3/2}$, $F' = 5$ Cs D_2 transition by modulation transfer spectroscopy (MTS)[33]. The wavelength-scale size of the waist at focus creates a dipole micro-trap of few-μm^3 volume. In the presence of cooler light, e.g. if the MOT is on, light-assisted collisions (LACs)[23] rapidly remove any pairs of atoms in this small volume. In practice, this ensures the presence of no more than one atom in the trap. The 852 nm FORT wavelength is sufficiently far from resonance as to produce little scattering by the trapped atom, yet close enough that a single aspheric lens can be diffraction limited when focusing both it and the spectroscopic wavelengths 780 nm (D_2) and 795 nm (D_1). 852 nm also coincides with the Cs D_2 line, which is convenient for frequency stabilization and atomic filtering. To position the dipole trap midway between the two lenses, a shearing interferometer (SI) is used to measure the beam divergence before the input lens, and after the output lens, and to set the divergences to be equal and opposite. The same SI is used in this symmetric condition to check for aberrations. For more details see 28.

Within the Gaussian beam approximation, the FORT potential is

$$U_{\mathrm{FORT}}(r,z) = \beta P_{\mathrm{FORT}} \frac{2}{\pi w^2(z)} \exp[-\frac{2r^2}{w^2(z)}] \qquad (1)$$

where $r = \sqrt{x^2+y^2}$ is the transverse radial coordinate, z is the axial coordinate, $\beta \approx -6.39 \times 10^{-36}$ Jm^{2}W^{-1} is the ground state light shift coefficient[34], P_{FORT} is the power of the FORT beam, $w(z) \equiv w_{\mathrm{FORT}}\sqrt{1+z^2/z_R^2}$ where w_{FORT} is the FORT beam waist, and $z_R \equiv \pi w_{\mathrm{FORT}}^2 / \lambda_{\mathrm{FORT}}$ is the Rayleigh length.

In most circumstances, the atom's thermal energy is far less than the trap depth $k_B T_{\mathrm{atom}} \ll U_0 \equiv |U_{\mathrm{FORT}}(0,0)|$, where k_B is the Boltzmann constant, and it is thus appropriate to use the harmonic approximation $U_{\mathrm{FORT}}(r,z) \simeq U_0[-1 + 2(r/w_{\mathrm{FORT}})^2 + (z/z_R)^2]$.

Fluorescence collection

The fluorescence collected by each lens is sent to a different channel of an avalanche photodiode detector (APD). Counts in each channel are recorded by an Arduino Due microcontroller and typically binned into 20 ms time bins. A representative signal is shown in the inset of the upper plot of Figure 3 (see *Underlying data*[35]). This shows a random telegraph

[1]Throughout, beam diameters indicate the diameter of the $1/e^2$ iso-intensity contour.

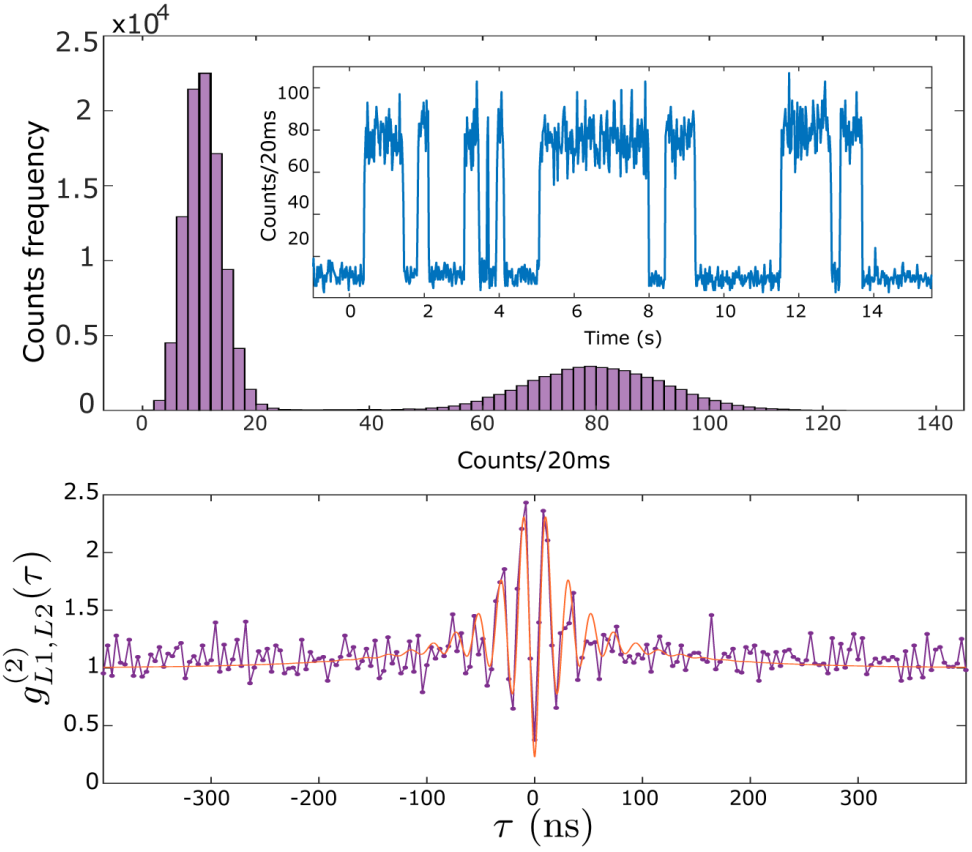


Figure 3. Single-atom resonance fluorescence. Upper plot: time series (inset) and histogram (main graph) of collected fluorescence from L1 as single atoms enter and leave the trap with magneto-optical trap (MOT) and far-off-resonance trap (FORT) in continuous operation, see text for details. Lower plot: normalized cross-correlation $g^{(2)}_{L1,L2}(\tau)$ between collection channels L1 and L2. Points show data, red curve shows a fit with $g^{(2)}_{L1,L2}(\tau) = 1 - A\exp[-|\tau|/\tau_1]\cos(\Omega'\tau) + B\exp[-|\tau|/\tau_2]$ with fitting parameters $\Omega' = 2\pi \times 47.6$ MHz, $\tau_1 = 28.5$ ns, $\tau_2 = 90.2$ ns, $A = 1.26$ and $B = 0.48$. This fit function is a heuristic approximation to the four-level $g^{(2)}(\tau)$ found numerically, for example in 34. See `HistogramAndNormalizedCrossCorrelation.csv` in *Underlying data*[35].

signal, i.e., stochastic switching between just two signal levels, corresponding to the zero-atom and one-atom conditions. The main figure of the upper plot shows a histogram of the counts of this telegraph signal for a measurement of 2700 s duration. It is clear that counts corresponding to zero atoms are well distinguishable from the counts corresponding to one atom in the trap. Due to LACs, larger atom numbers are not observed. We use this real-time telegraph signal for fine alignment of the collection fibers to the atom. The clear gap in counts allows us to perform sequence measurements triggered by the presence of an atom in the trap. The lower plot in Figure 3 shows the normalized cross-correlation $g^{(2)}_{L1,L2}(\tau)$ of the signals collected via L1 and L2 (see *Underlying data*[35]). Antibunching, i.e. $g^{(2)}_{L1,L2}(0) < 1$, indicates a non-classical photon flux typical of single-emitter systems. A number of departures from the ideal two-level $g^{(2)}_{L1,L2}(\tau)$ function, previously noted in the literature, can be observed here: $g^{(2)}_{L1,L2}(0)$ is not zero, due to background light, here dominated by MOT fluorescence [28, Figure 1]. The maximum of $g^{(2)}_{L1,L2}(\tau)$ is not 2, due to shuttling of the state between the $F = 1$ and $F = 2$ ground states by the cooling and repumper beams[36]. At the largest delays shown here, for which $|\tau| \gg 1/\Gamma_0$, $g^{(2)}_{L1,L2}(\tau)$ is somewhat larger than unity. This may be explained by slow fluctuations in trap loading efficiency.

Trap characterization

Characterization of the imaging optics of the MCG have been extensively described in 28. In this section we report several characteristics that have not been previously reported, principally characteristics of the trapped atoms. To the extent possible, we have attempted to follow established protocols, to facilitate comparison with prior and existing experimental setups.

Occupancy and loading rate

With the MOT running, an atom can be lost from the FORT by LAC with the next atom to be captured by the FORT, or by one-atom loss processes, e.g., collision with a background gas

molecule[37]. Writing the respective rates as R_{cap} and R_{1BL}, the net rate $R_{cap} + R_{1BL} \approx 0.36\ s^{-1}$ is observed in the data of Figure 3. The ratio $R_{1BL}/R_{cap} = P_0/P_1 - 1$, where P_0 and P_1 are the steady-state probabilities for the trap to contain zero or one atom, respectively. These probabilities can be found by integrating the respective peaks that appear in Figure 3 (upper part, main), to find $P_0/P_1 \approx 2$, and thus $R_{1BL} \approx R_{cap} \approx 0.18\ s^{-1}$. These observations are specific to the conditions that held when those data were taken, and can be adjusted to suit the needs of a particular experiment. The capture rate R_{cap} depends on the conditions of the MOT and FORT, and can be conveniently controlled using the MOT compensation coils to displace the MOT relative to the FORT. The one-body loss rate R_{1BL} depends on the background gas pressure, and can be controlled by introducing more Rb vapor into the chamber by heating the Rb dispenser.

Trap lifetime

By turning off the MOT beams when an atom's fluorescence is detected on the APD, it is possible to trap and hold an atom in the FORT without loss by LAC. In this situation atoms can still be lost by collisions with background gas in the vacuum chamber, and by heating from stray light, scattering of the FORT beam, or FORT power or pointing fluctuations. The lifetime of an atom due to these effects was measured, the results of which are presented *Underlying data*[35] and shown in Figure 4. The observed lifetime of 3.5(3) s is typical in our setup. The lifetime decreases with increasing pressure in the vacuum chamber, for example when dispensers are heated to release Rb. This suggests that the loss is principally from collisions with background Rb atoms.

FORT beam waist

The FORT beam waist w_{FORT}, together with the FORT power, determines the shape of the trapping potential, including the trap depth. Other measurements require knowledge of this trapping potential, e.g. the measurement of temperature by the release-and-recapture method[38].

The FORT power can be directly measured outside of the vacuum chamber without great difficulty. w_{FORT} can be calculated based on the geometry of the FORT beam outside of the vacuum chamber and the optical properties of the high-NA lens that focuses it. In this strongly-focused scenario, however, w_{FORT} is sensitive to aberrations, which could be introduced by the vacuum windows or by the lenses themselves. Such aberrations are difficult to measure, especially *in situ*. Using our input beam diameter and computing the beam waist by gaussian beam optics and the thin-lens approximation, assuming no aberrations, gives the result $w_{FORT} = 1.2\mu m$, which we take as a lower limit. Parametric excitation (PE) of the atomic centre of mass motion is a proven method to determine w_{FORT} in trapped ensembles. PE heats the ensemble, leading to an observable loss of atoms from the trap[39,40]. Although this method has been applied to single trapped atoms[41–43], its interpretation is complicated by the fact that, unlike an ensemble, a single atom does not thermalize. In section **Parametric resonances and trap frequency** we present PE measurements, which by a naïve interpretation imply a $w_{FORT} = 1.75\ \mu m$. A comparison against Monte Carlo (MC) simulation of the PE process, described in section **Parametric resonances and trap frequency**, indicates a value closer to $w_{FORT} = 1.5\ \mu m$, while also suggesting that other factors such as non-parametric heating are important.

Considering the above, w_{FORT} is only weakly constrained, to the range 1.2μm to 1.75μm. Rather than carry this ambiguity through the rest of the article, we use a nominal value $w_{FORT} = 1.6\mu m$ for the calculations and measurements in the sections that follow. For this value of w_{FORT}, the transverse and

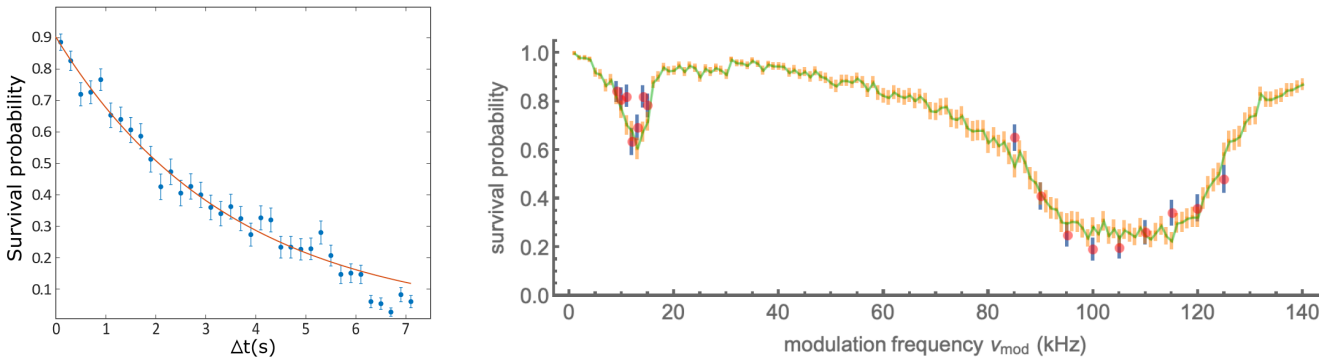


Figure 4. Removal of atoms from the trap with and without parametric excitation. Left: Persistence of a trapped atom in the far-off-resonance trap (FORT) as a function of hold time Δt. After detection of an atom by fluorescence, the magneto-optical trap (MOT) beams are turned off and the magnetic field gradient reduced, to prevent capture of a second atom in the FORT. After at time Δt, the MOT beams are restored, and the presence or absence of the atom inferred from the fluorescence it produces. Each point shows the average of 150 trials, error bars show ± one standard error assuming binomial statistics. Line shows exponential fit with $1/e$ lifetime 3.5(3) s. See data file `Lifetime.csv` in *Underlying data*[35]. Right: Survival probability of an atom in the presence of parametric excitation at modulation frequency ν_{mod}, as described in the text. Data (simulation) are shown as red (green) points. Error bars indicate ± one standard error assuming binomial statistics. See data file `SurvivalVersusModulationFrequency.csv` and simulation code file `SingleAtomParametricExcitation.jl` in *Underlying data*[35].

axial trap frequencies are then $\omega_r = \sqrt{4U_0 / m_{87} w_{\mathrm{FORT}}^2} \approx 56$ kHz and $\omega_z = \sqrt{2U_0 / m_{87} z_R^2} \approx 6.7$ kHz, respectively, where m_{87} is the ^{87}Rb mass.

Parametric resonances and trap frequency

Parametric excitation, in which the FORT power is modulated to excite parametric resonances in the atomic motion, is widely used to characterize the trap frequencies in optically-trapped atomic gases[39,40]. With ensembles, the heating rate and thus the rate of loss from the trap show resonances at specific frequencies. In the harmonic approximation, these occur at double the trap frequencies, due to the even symmetry of the perturbation to the potential. Corrections due to trap anharmonicity have been studied[39] and the technique has been applied to single atoms[41].

To measure these parametric resonances we used the following sequence: after loading an atom, we blocked the cooler light, leaving on the FORT and repumper beams, so the atom remained in the now-dark $F = 2$ manifold. We then modulated the FORT power P_{FORT} for time t_{mod} at a modulation frequency ν_{mod} with a depth of modulation of $\approx 20\%$ in the higher-frequency range and $\approx 35\%$ in the lower. The power modulation was accomplished by sinusoidally modulating the amplitude of the radio frequency (RF) voltage that drives the FORT acousto-optic modulator and thus the power of the first diffraction order into a single-mode fibre that leads to the experiment.

Following the trap modulation, we checked for the presence of the atom by turning on again the cooler and collecting fluorescence. We repeated this process for 100 atoms for values of ν_{mod} near the second harmonic of the 6.7 kHz longitudinal and 56 kHz transverse trap frequencies predicted for the trap potential with the nominal waist $w_0 = 1.6$μm. The modulation was maintained for 150 ms in the lower-frequency range and 30 ms in the higher. Results are shown in Figure 4, with resonances at $\approx$ 12kHz and $\approx$ 100kHz, about 10% lower than expected based on the nominal trap frequencies, although the broad and asymmetric profile of the loss feature makes any frequency assignment imprecise. In the naïve interpretation of the technique, in which the transverse resonance frequency obeys $\omega_r \propto w_{\mathrm{FORT}}^{-1}$, this would indicate $w_0 \approx 1.75$μm.

To understand better these observations, we studied the PE process by MC simulation, in which atoms drawn from a Boltzmann distribution (see section **Atom temperature**) are allowed to evolve under the modulated potential, Equation 1 with harmonically oscillating P_{FORT}. These simulations show that the PE process *per se* is not capable of resonantly heating a single atom out of the trap. This is because the combination of phase-sensitive amplification and trap anharmonicity leads first to an excitation of motion along the resonant axes, phase-shifting due to anharmonicity, and then de-excitation of the same trap motion. This contrasts strongly with the case for trapped ensembles, in which PE plus collisional energy redistribution produces irreversible heating. Nonetheless, the simulations indicate that inclusion of a stochastic element in the PE process can reproduce the main features of the observed survival probability data. To obtain the MC results shown in Figure 4, we included in the dynamics a Langevin term describing isotropic momentum-space diffusion, as would be created by scattering of resonant stray light, near-resonant rempumper light, or far-off-resonance FORT light. The combined effect of near-resonant light with FORT light can result in stronger heating than predicted by simple photon recoil of these same sources[44,45]. Adjustment of the simulation parameters "by hand" finds best agreement with a trap waist $w_{\mathrm{FORT}} = 1.47$μm, modulation depth of 30% (22%) and heating rate of 2.5 recoil/ms (6.5 recoil/ms) below (above) 30 kHz. It is clear that the accurate interpretation of single-atom PE data is a non-trivial task, and we do not consider this result, absent a fuller characterization of the excitation process, to give a reliable value for w_{FORT}.

Atom temperature

We use the release and recapture method to determine the atom's temperature in the FORT (see *Underlying data*[35]), as illustrated in Figure 5a. We follow the protocol and analysis described in 38. The MOT and FORT are run until an atom is detected by its resonance fluorescence, as described above. Repumper and cooler beams are then turned off and the MOT magnetic gradient reduced to prevent a second atom from falling into the trap. The FORT is then turned off for a time Δt, during which the atom can escape the FORT by ballistic motion. We then turn on the FORT, wait 100 ms and turn on the MOT beams. A recaptured atom is detected by the fluorescence it produces in this last phase. The wait time is introduced to ensure a temporal separation, by multiple recording time bins, of the fluorescence counts before and after the release and recapture modulation of the FORT. This avoids possible systematic errors associated with synchronization of the optical beams to the data acquisition. We repeat this sequence 100 times for each value of Δt. In Figure 5b we show the recaptured fraction $P_R(\Delta t)$ for typical conditions.

We compare the experimental observations against a MC simulation of the atom's probability to be recaptured. In this simulation we assume that, at the moment the FORT is turned off, the atom's position is gaussian-distributed about the trap center, with zero mean and variances $\langle \Delta x^2 \rangle = \langle \Delta y^2 \rangle = k_B T/(m_{87}\omega_r^2)$ and $\langle \Delta z^2 \rangle = k_B T/(m_{87}\omega_z^2)$, which follow from the equipartition theorem under the potential in the harmonic approximation. We assume the atom's momentum distribution has zero mean and variance $\left\langle \Delta v_{x,y,z}^2 \right\rangle = k_B T/m_{87}$, which describes the Maxwell-Boltzmann distribution. We then compute the evolved position $\mathbf{x}_f = \mathbf{x}(t = \Delta t)$ and velocity $\mathbf{v}_f = \mathbf{v}(t = \Delta t)$ after ballistic flight under gravity for time Δt, and the resulting total energy $E_T \equiv m_{87}\mathrm{v}_f^2/2 + U_{\mathrm{FORT}}(\mathbf{x}_f)$ when the FORT is turned on at time Δt. If $E_T < 0$, the atom is considered recaptured.

For given T and Δt, we repeat this sequence 100 times to find the recaptured fraction $f_R(T, \Delta t)$. To compare the simulation and experimental results, we calculate $\chi^2(T) = \sum_{\Delta t} [f_R(T, \Delta t) - P_R(\Delta t)]^2/\sigma^2(\Delta t)$, where $\sigma(\Delta t)$ is the standard error of $P_R(\Delta t)$. As

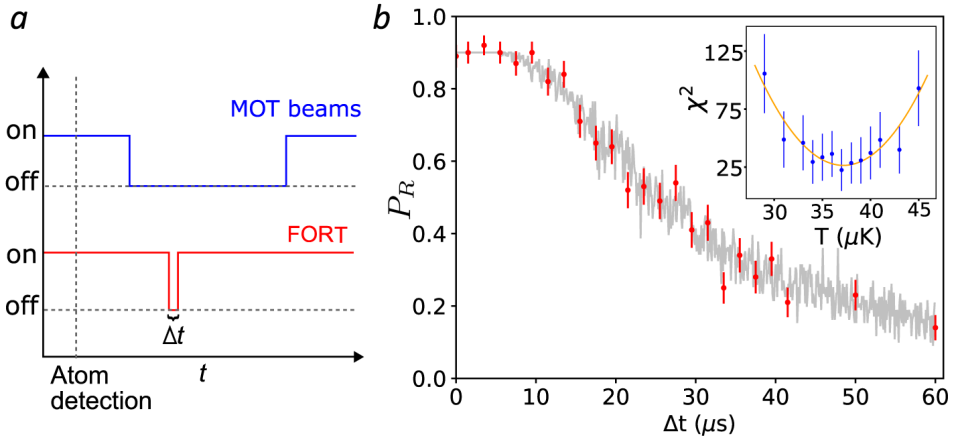


Figure 5. Release and recapture measurement of atom temperature. a. Cooling, repumper and far-off-resonance trap (FORT) beams temporal sequence (not to scale). **b**. Observed recaptured fraction P_R as a function of the release time Δt (red circles). Each point is the result of 100 trials. Error bars show ± one standard error of P_R assuming a binomial distribution. Grey points show the recapture frequencies observe in a Monte Carlo (MC) simulation with T_{atom} = 37μK, and including a Δt-independent 11 percent probability of losing the atom between recapture and fluorescence detection. Inset: χ^2 distance between data and MC simulation (blue circles) for different temperatures T. Error bars show ± one standard error of χ^2 by propagation of error. A least-squares quadratic fit $\chi^2_{fit}(T)$ (orange curve, see text) finds T_{atom} = 37(2) μK. MOT: magneto-optical trap. See `Temperature.csv` in *Underlying data*[35].

shown in Figure 5b (inset), we compute $\chi^2(T)$ for several T and fit, by least squares, a quadratic function which we denote $\chi^2_{fit}(T)$. The minimum of $\chi^2_{fit}(T)$ is taken as the best-guess temperature T_{atom} = 37(2) μK, with uncertainty $\sqrt{2\left\lfloor \partial^2\chi^2_{fit}(T)/\partial^2 T\right\rfloor^{-1}}$, where $\left\lfloor \partial^2\chi^2_{fit}(T)/\partial^2 T\right\rfloor$ is the 1-σ lower confidence bound on $\partial^2\chi^2_{fit}(T)/\partial^2 T$[46]. We note that $T_{atom} \ll U_0/k_B \approx$ 780 μK, which justifies the harmonic approximation to the trapping potential.

Collection-efficiency mapping using stochastic loading

The selectivity in the collection at a right-angle to the trap axis is one of the advantages for the MCG, and provides more access channels when working in the single atom regime. Here we show a correlation-based technique to map the collection of this right-angle access (see *Underlying data*[35]). We first produce a 1D optical lattice potential by reflecting the FORT light back through lens L2 in order to create a standing wave, as shown in Figure 6a. The input FORT power is reduced to 2.5 mW to partially compensate the intensity boost implied by the standing wave geometry. Atoms were randomly loaded from the free-running MOT into the lattice, and their fluorescence recorded with a camera via lens L3. The camera has a pixel size of 6.45μm × 6.45μm, corresponding to 1μm/pixel at the atoms. Simultaneously, light collected by L1 (along the lattice axis) and L4 (at a right angle) are coupled into single-mode fibers and detected with APDs.

As shown in Figure 6d, the video records the capture and loss of many atoms at different lattice locations. Spatially-resolved correlation of individual pixels with the L1 and L4 APD signals is then used to measure the spatial distribution of collection efficiency when collecting both along and transverse to the trap axis. Specifically, if $I_i(t_n)$ is the stripe-averaged intensity at pixel i at time t_n, and $R^{(L)}(t_n)$ is the observed rate of photon detections behind lenses $L \in \{L1, L4\}$ at that same time, then a general linear model is

$$R_C^{(L)}(t_n) = \sum_i C_i^{(L)} I_i(t_n) \qquad (2)$$

where $C_i^{(L)}$ is the time-independent coupling efficiency from pixel i to lens L. Using the data shown in Figure 6, we find $C_i^{(L)}$ by linear regression, i.e., by minimizing the square error $\sum_n \left[R_C^{(L)}(t_n) - R^{(L)}(t_n)\right]^2$, which is to say we make a least-squares fit with $\{C_i^{(L)}\}$ as the fit parameters. As expected, and as shown in Figure 6i, the L4 collection is concentrated in a region of FWHM ≈ 2 μm in the camera image, whereas the L1 collection efficiency shows a broad peak spread over many pixels.

Assuming that L1 collects a Gaussian beam, the coupling efficiencies $C_i^{(L1)}$ should describe a Lorentzian function of z, and thus of i, with FWHM of $2z_R$, where $z_R = \pi w_0^2/\lambda \approx 10$ μm=10 pixel is the Rayleigh length and w_0 is the waist of L1 at focus. We note that this Lorentzian shape plausibly describes $C_i^{(L1)}$ but that any fit to $C_i^{(L1)}$ would be offset by ≈ 5 pixel from the centre of $C_i^{(L4)}$. This offset can be explained as simply an imperfect focusing of L1.

For comparison, Figure 6b and c show collection with lenses L1 and L4 with the single trap described in section **System description**. With no optical lattice, collection in the two

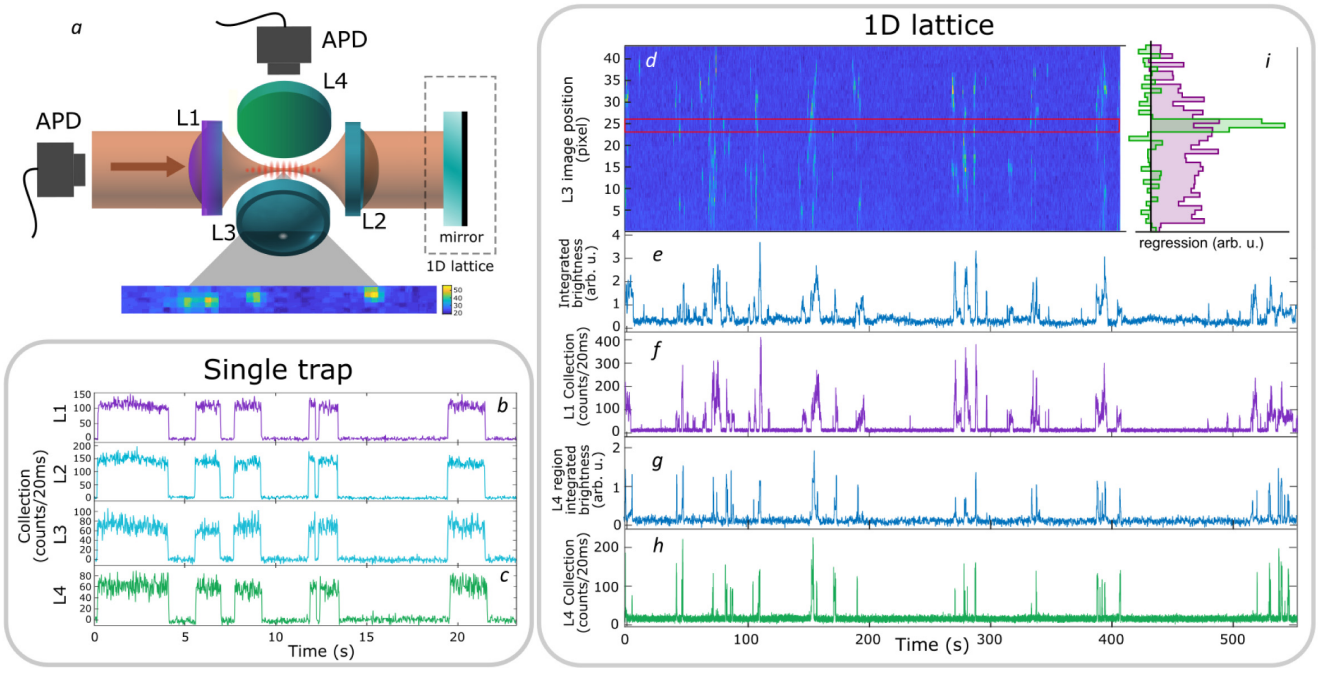


Figure 6. Localized collection of light from a simple far-off-resonance trap (FORT) and a 1D lattice. a: Geometry of the trap, collection, and imaging optics. **b** (**c**): fluorescence signals collected by L1 (L4) of the simple FORT, i.e., with no retro-reflected beam, as seen on avalanche photodiode detectors (APDs). Collection by L2 and L3 lenses is also shown for comparison. The collection efficiency of L3 and L4 is reduced relative to L1 and L2 due to the asymmetric nature of the trap - an atom that moves along the trap axis can leave the region collected by L3 and L4, while remaining in the region collected by L1 and L2. **d**: spatially-resolved fluorescence over time from a continuously-loaded 1D optical lattice, imaged through L3 on a charge-coupled device (CCD) camera. The camera image shows a tilting with respect to the array, related with the camera positioning. Vertical axis shows axial position in the lattice in pixels, at a magnification of 1 pixel/μm, horizontal axis shows time of acquisition. Colors indicate fluorescence intensity (arb. u.) integrated over a stripe of transverse dimension 5 pixel about the trap axis, increasing from dark to light. The same fluorescence signal is shown integrated over the length of the lattice in **e** and over the pixels between red lines in **g**. **f** (**h**): Single-mode fluorescence collection by L1 (L4). **i** Contribution of different lattice locations (vertical axis, pixels on same scale as **d**) to the L1 (purple) and L4 (green) signals (horizontal axis). Values determined by linear regression, i.e. least-squares fit of a linear combination of camera pixel signals to the L1 and L4 APD signals (see text). See also `RightAngleCollection.csv` in *Underlying data*[35].

directions is strongly correlated because each trapped atom explores the entire trap volume, and each channel presents a good signal-to-noise ratio.

Conclusion

We have described a system for stable, long-term trapping and cooling of single ^{87}Rb atoms at the center of a Maltese cross geometry optical system of four high-NA aspheric lenses in vacuum. The system gives high-NA access to the common focal region, which we demonstrate by simultaneously coupling two FORT trapping beams, two single-mode collection fibers, and a high-NA imaging system to observe spatio-temporal atom-number correlations, from which we determine the spatially-resolved single-mode collection efficiencies in the trap-axial and trap-transverse directions. We have studied the principal characteristics of this trapping system, including the loading dynamics, trap lifetime, visibility of single-atom signals, in-trap atom temperature and parametric excitation spectrum. We find trap performance comparable to what has been reported for single-atom traps with one- or two-lens optical systems. We conclude that the multi-directional high-NA access provided by the Maltese cross geometry can be achieved while preserving other trap characteristics such as lifetime, temperature, and trap size.

Data availability

Underlying data

Zenodo: Manipulating and measuring single atoms in the Maltese cross geometry - Data.

https://doi.org/10.5281/zenodo.5118863[35].

This project contains the following underlying data:

- `HistogramAndNormalizedCrossCorrelation.csv` (single atom resonance fluorescence histogram, time series (inset) and normalized cross-correlation in Figure 3).

- `Lifetime.csv` (removal of atoms from the trap without parametric excitation in Figure 4 (left)).
- `SurvivalVersusModulationFrequency.csv` (removal of atoms from the trap with parametric excitation in Figure 4 (right)).
- `Temperature.csv` (release and recapture measurement of atom temperature in Figure 5).
- `RightAngleCollection.csv` (localized collection of light from a single far-off-resonance trap and a 1D lattice in Figure 6).
- `SingleAtomParametricExcitation.jl` (Monte Carlo simulation code of the parametric excitation process in Figure 4 (right)).

Data are available under the terms of the Creative Commons Attribution 4.0 International license (CC-BY 4.0).

Acknowledgements

The authors thank Ludovic Brossard, Antoine Browaeys and Vindhiya Prakash for helpful discussions.

References

1. Bergamini S, Darquié B, Jones M, *et al.*: **Holographic generation of microtrap arrays for single atoms by use of a programmable phase modulator.** *J Opt Soc Am B.* 2004; **21**(11): 1889–1894.
Publisher Full Text
2. Barredo D, de Léséleuc S, Lienhard V, *et al.*: **An atom-by-atom assembler of defect-free arbitrary two-dimensional atomic arrays.** *Science.* 2016; **354**(6315): 1021–1023.
PubMed Abstract | Publisher Full Text
3. Schrader D, Dotsenko I, Khudaverdyan M, *et al.*: **Neutral atom quantum register.** *Phys Rev Lett.* 2004; **93**(15): 150501.
PubMed Abstract | Publisher Full Text
4. Kaufman AM, Lester BJ, Regal CA: **Cooling a Single Atom in an Optical Tweezer to Its Quantum Ground State.** *Phys Rev X.* 2012; **2**(4): 041014.
Publisher Full Text
5. Volz J, Weber M, Schlenk D, *et al.*: **Observation of Entanglement of a Single Photon with a Trapped Atom.** *Phys Rev Lett.* 2006; **96**(3): 030404.
PubMed Abstract | Publisher Full Text
6. Liu LR, Hood JD, Yu Y, *et al.*: **Building one molecule from a reservoir of two atoms.** *Science.* 2018; **360**(6391): 900–903.
PubMed Abstract | Publisher Full Text
7. Tey MK, Maslennikov G, Liew TCH, *et al.*: **Interfacing light and single atoms with a lens.** *New J Phys.* 2009; **11**: 043011.
Publisher Full Text
8. Chin YS, Steiner M, Kurtsiefer C: **Nonlinear photon-atom coupling with 4Pi microscopy.** *Nat Commun.* 2017; **8**(1): 1200.
PubMed Abstract | Publisher Full Text | Free Full Text
9. Aljunid SA, Tey MK, Chng B, *et al.*: **Phase Shift of a Weak Coherent Beam Induced by a Single Atom.** *Phys Rev Lett.* 2009; **103**(15): 153601.
PubMed Abstract | Publisher Full Text
10. Tey MK, Chen Z, Aljunid SA, *et al.*: **Strong interaction between light and a single trapped atom without the need for a cavity.** *Nature Phys.* 2008; **4**: 924–927.
Publisher Full Text
11. Leong V, Seidler MA, Steiner M, *et al.*: **Time-resolved scattering of a single photon by a single atom.** *Nat Commun.* 2016; **7**: 13716.
PubMed Abstract | Publisher Full Text | Free Full Text
12. Slodička L, Hétet G, Gerber S, *et al.*: **Electromagnetically Induced Transparency from a Single Atom in Free Space.** *Phys Rev Lett.* 2010; **105**(15): 153604.
PubMed Abstract | Publisher Full Text
13. Kaufman AM, Lester BJ, Reynolds CM, *et al.*: **Two-particle quantum interference in tunnel-coupled optical tweezers.** *Science.* 2014; **345**(6194): 306–9.
PubMed Abstract | Publisher Full Text
14. Lester BJ, Lin Y, Brown MO, *et al.*: **Measurement-Based Entanglement of Noninteracting Bosonic Atoms.** *Phys Rev Lett.* 2018; **120**(19): 193602.
PubMed Abstract | Publisher Full Text
15. Kaufman AM, Lester BJ, Foss-Feig M, *et al.*: **Entangling two transportable neutral atoms via local spin exchange.** *Nature.* 2015; **527**(7577): 208–11.
PubMed Abstract | Publisher Full Text
16. Saffman M, Walker TG, Mølmer K: **Quantum information with Rydberg atoms.** *Rev Mod Phys.* 2010; **82**(3): 2313.
Publisher Full Text
17. Bernien H, Schwartz S, Keesling A, *et al.*: **Probing many-body dynamics on a 51-atom quantum simulator.** *Nature.* 2017; **551**(7682): 579–584.
PubMed Abstract | Publisher Full Text
18. Labuhn H, Barredo D, Ravets S, *et al.*: **Tunable two-dimensional arrays of single Rydberg atoms for realizing quantum Ising models.** *Nature.* 2016; **534**(7609): 667–70.
PubMed Abstract | Publisher Full Text
19. Asenjo-Garcia A, Moreno-Cardoner M, Albrecht A, *et al.*: **Exponential Improvement in Photon Storage Fidelities Using Subradiance and "Selective Radiance" in Atomic Arrays.** *Phys Rev X.* 2017; **7**(3): 031024.
Publisher Full Text
20. Perczel J, Borregaard J, Chang DE, *et al.*: **Topological Quantum Optics in Two-Dimensional Atomic Arrays.** *Phys Rev Lett.* 2017; **119**(2): 023603.
PubMed Abstract | Publisher Full Text
21. Glicenstein A, Ferioli G, Šibalić N, *et al.*: **Collective Shift in Resonant Light Scattering by a One-Dimensional Atomic Chain.** *Phys Rev Lett.* 2020; **124**(25): 253602.
PubMed Abstract | Publisher Full Text
22. Rui J, Wei D, Rubio-Abadal A, *et al.*: **A subradiant optical mirror formed by a single structured atomic layer.** *Nature.* 2020; **583**(7816): 369–374.
PubMed Abstract | Publisher Full Text
23. Schlosser N, Reymond G, Protsenko I, *et al.*: **Sub-poissonian loading of single atoms in a microscopic dipole trap.** *Nature.* 2001; **411**(6841): 1024–1027.
PubMed Abstract | Publisher Full Text
24. Sortais YRP, Marion H, Tuchendler C, *et al.*: **Diffraction-limited optics for single-atom manipulation.** *Phys Rev A.* 2007; **75**(1): 013406.
Publisher Full Text
25. Nogrette F, Labuhn H, Ravets S, *et al.*: **Single-Atom Trapping in Holographic 2D Arrays of Microtraps with Arbitrary Geometries.** *Phys Rev X.* 2014; **4**(2): 021034.
Publisher Full Text
26. Martinez-Dorantes M, Alt W, Gallego J, *et al.*: **State-dependent fluorescence of neutral atoms in optical potentials.** *Phys Rev A.* 2018; **97**(2): 023410.
Publisher Full Text
27. Martinez-Dorantes M: **Fast non-destructive internal state detection of neutral atoms in optical potentials.** Ph.D. thesis, Rheinischen Friedrich Wilhelms Universitaet Bonn, 2016.
Reference Source
28. Bruno N, Bianchet LC, Prakash V, *et al.*: **Maltese cross coupling to individual cold atoms in free space.** *Opt Express.* 2019; **27**(21): 31042–31052.
PubMed Abstract | Publisher Full Text
29. Glicenstein A, Ferioli G, Brossard L, *et al.*: **Fast and efficient preparation of 1D chains and dense cold atomic clouds.** *arXiv e-prints.* 2021.
Reference Source
30. Jennewein S, Besbes M, Schilder NJ, *et al.*: **Coherent Scattering of Near-Resonant Light by a Dense Microscopic Cold Atomic Cloud.** *Phys Rev Lett.* 2016; **116**(23): 233601.
PubMed Abstract | Publisher Full Text
31. Goncalves D, Mitchell MW, Chang DE: **Strong quantum correlations of light emitted by a single atom in free space.** *arXiv e-prints.* arXiv:2004.01993, 2020; **2004**: 01993.
Reference Source
32. Glicenstein A, Ferioli G, Brossard L, *et al.*: **Preparation of one-dimensional**

chains and dense cold atomic clouds with a high numerical aperture four-lens system. *Phys Rev A.* 2021; **103**(4): 043301.
Publisher Full Text

33. Martinez de Escobar YN, Álvarez SP, Coop S, *et al.*: **Absolute frequency references at 1529 and 1560 nm using modulation transfer spectroscopy.** *Opt Lett.* 2015; **40**(20): 4731–4734.
PubMed Abstract | **Publisher Full Text**

34. Coop S, Palacios S, Gomez P, *et al.*: **Floquet theory for atomic light-shift engineering with near-resonant polychromatic fields.** *Opt Express.* 2017; **25**(26): 32550–32559.
Publisher Full Text

35. Bianchet LC: **Manipulating and measuring single atoms in the Maltese cross geometry Data.** [Data set], *Zenodo.* 2021.
http://www.doi.org/10.5281/zenodo.5118863

36. Volz J, Weber M, Schlenk D, *et al.*: **An atom and a photon.** *Laser Phys.* 2007; **17**: 1007–1016.
Publisher Full Text

37. Schlosser N, Reymond G, Grangier P: **Collisional Blockade in Microscopic Optical Dipole Traps.** *Phys Rev Lett.* 2002; **89**(2): 023005.
PubMed Abstract | **Publisher Full Text**

38. Tuchendler C, Lance AM, Browaeys A, *et al.*: **Energy distribution and cooling of a single atom in an optical tweezer.** *Phys Rev A.* 2008; **78**(3): 033425.
Publisher Full Text

39. Wu J, Newell R, Hausmann M, *et al.*: **Loading dynamics of optical trap and parametric excitation resonances of trapped atoms.** *J Appl Phys.* 2006; **100**(5): 054903.
Publisher Full Text

40. Scheunemann R, Cataliotti FS, Hänsch TW, *et al.*: **Resolving and addressing atoms in individual sites of a CO_2-laser optical lattice.** *Phys Rev A.* 2000; **62**(5): 051801.
Publisher Full Text

41. Shih CY, Chapman MS: **Nondestructive light-shift measurements of single atoms in optical dipole traps.** *Phys Rev A.* 2013; **87**(6): 063408.
Publisher Full Text

42. Shih CY: **Characterizing single atom dipole traps for quantum information applications.** Ph.D. thesis, Georgia Institute of Technology, 2013.
Reference Source

43. Brossard L: **Study of light-induced dipolar interactions in cold atoms assemblies.** Ph.D. thesis, Université Paris-Saclay, 2020.
Reference Source

44. Dalibard J, Cohen-Tannoudji C: **Dressed-atom approach to atomic motion in laser light: the dipole force revisited.** *J Opt Soc Am B.* 1985; **2**(11): 1707–1720.
Publisher Full Text

45. Vanderbruggen T, Mitchell MW: **Near-resonant optical forces beyond the two-level approximation for a continuous source of spin-polarized cold atoms.** *Phys Rev A.* 2013; **87**: 033410.
Publisher Full Text

46. Bevington PR, Robinson DK: **Data Reduction and Error Analysis for the Physical Sciences.** 3rd ed. McGrawHill, NY, 2003.
Reference Source

Open Peer Review

Current Peer Review Status: ✔ ✔

Version 1

Reviewer Report 18 October 2021

https://doi.org/10.21956/openreseurope.15058.r27739

© **2021 Nguyen C et al.** This is an open access peer review report distributed under the terms of the Creative Commons Attribution License, which permits unrestricted use, distribution, and reproduction in any medium, provided the original work is properly cited.

✔ **Chi Huan Nguyen**
Centre for Quantum Technologies, National University of Singapore, Singapore, Singapore
Chang Hoong Chow
Centre for Quantum Technologies, Singapore, Singapore

In this manuscript, Bianchet *et. al* report a detailed study of single neutral atoms trapped in a four-lens arrangement known as the Maltese cross geometry (MCG). In particular, the authors characterize the loading rate, lifetime, and temperature of the single trapped atoms as well as the photon statistics of the fluorescence.

The four lenses have high numerical apertures allowing four-directional coupling to the single atoms. The setup can therefore obtain strong coupling between single photons and single atoms making it a potential candidate for building up quantum networks. In addition, the MCG system is also useful in experiments that involve disordered ensembles and atomic arrays. In this case, the orthogonal pair of lenses provides the additional selectivity of photon collections at a right-angle to the trap axis.

Overall, the paper is well written and easy to understand. The figures are produced with high quality. We strongly recommend indexing the manuscript. We have some minor comments and questions:

1. The authors presented the microtrap characterization, motivated by the suspicion that the incorporation of a third and fourth lens might have degraded the trapping ability of the system, which is likely not the case for neutral atoms. What is the physical intuition behind this conjecture?

2. We think it is helpful that the authors can provide an estimate of the solid angle covered by four lenses in the manuscript.

3. As there is not much access to the centre of the 4 lenses on the trapping plane, where is the Rb oven with respect to the trapping zone? Does the atomic beam come from the top or

the bottom?

4. As shown in Figure 5.a, there is a delay between the switching on of the FORT and MOT beams. Could the author explain this point in the manuscript?

5. It would be great if the authors could comment more on the background level in the g2 correlation between the collection from L1 and L2. Are they referring to the small offset from 1 at a longer timescale?

6. As shown in the inset of Figure 5.a, the CCD camera image of the atoms trapped in the 1D lattice exhibits a significant tiltness with respect to the camera's horizon axis. Is it because of the angular misalignment of the optical axes of the two pairs of lenses?

7. When coupling fluorescence from the 1D lattice into a single-mode fiber through L4 lens, does the collection region of FWHM ~ 2um agree with the numerical aperture of the collection optics?

Is the work clearly and accurately presented and does it cite the current literature?
Yes

Is the study design appropriate and does the work have academic merit?
Yes

Are sufficient details of methods and analysis provided to allow replication by others?
Yes

If applicable, is the statistical analysis and its interpretation appropriate?
Yes

Are all the source data underlying the results available to ensure full reproducibility?
Yes

Are the conclusions drawn adequately supported by the results?
Yes

Competing Interests: No competing interests were disclosed.

Reviewer Expertise: single atom traps, light-matter interaction, ion trap, quantum computing, quantum optics.

We confirm that we have read this submission and believe that we have an appropriate level of expertise to confirm that it is of an acceptable scientific standard.

Author Response 04 Feb 2022

Lorena C Bianchet

We thank Drs. Nguyen and Chow for their insightful questions and suggestions. Specific replies are given below.

CHN&CHC Point 1: The authors presented the microtrap characterization, motivated by the suspicion that the incorporation of a third and fourth lens might have degraded the trapping ability of the system, which is likely not the case for neutral atoms. What is the physical intuition behind this conjecture?
Reply: The incorporation of a second pair of lenses in the system implies less optical access for the MOT beams, which translates into less alignment freedom, smaller MOT beams and/or more light scattered from the edges of the lenses. There is little published work on very small MOTs, but it is clear that the trapping power of the MOT is a strong function of beam size, so that using extremely small beams to eliminate the possibility of scattered light is not appealing. These same beams act to cool an atom that falls into the FORT. While a reduction in the ~mm size of the MOT beams is not expected to significantly change the optical conditions experienced by an atom in the ~μm sized FORT, an increase in scattered light implies a fluctuating powers and polarizations as seen by the atom. This is the physical intuition behind the conjecture. Other groups have, via personal communications, reported that a system with four high-NA lenses was more difficult to operate than a comparable system with two high-NA lenses.

CHN&CHC Point 2: *We think it is helpful that the authors can provide an estimate of the solid angle covered by four lenses in the manuscript.*
Reply: We have added an estimate to the revised manuscript.

CHN&CHC Point 3: As there is not much access to the centre of the 4 lenses on the trapping plane, where is the Rb oven with respect to the trapping zone? Does the atomic beam come from the top or the bottom?
Reply: The MOT is loaded, not from a beam, but rather from the residual Rb vapor in the vacuum chamber. This is produced by a dispenser located approximately 10 cm below the plane that contains the lenses and other optics shown in Figure 2.

CHN&CHC Point 4: As shown in Figure 5.a, there is a delay between the switching on of the FORT and MOT beams. Could the author explain this point in the manuscript?
Reply: This delay is not essential to the technique, but simplifies the data analysis. By including this delay, there is no ambiguity about what fluorescence events are from before the release/recapture modulation of the FORT, and which are from after. It allows us to apply consistently a threshold-based analysis of the observed fluorescence counts to identify recaptured atoms even at short release times.

CHN&CHC Point 5: It would be great if the authors could comment more on the background level in the g2 correlation between the collection from L1 and L2. Are they referring to the small offset from 1 at a longer timescale?
Reply: We have expanded the discussion of the g2 correlation function.

CHN&CHC Point 6: As shown in the inset of Figure 5.a, the CCD camera image of the atoms trapped in the 1D lattice exhibits a significant tiltness with respect to the camera's horizon axis. Is it because of the angular misalignment of the optical axes of the two pairs of lenses?

Reply: This is simply because of an unintended tilting of the camera that was used to acquire the image. We have added an explanation to the revised article.

CHN&CHC Point 7: When coupling fluorescence from the 1D lattice into a single-mode fiber through L4 lens, does the collection region of FWHM ~ 2um agree with the numerical aperture of the collection optics?
Reply: We believe the question concerns the width of the green correlation function in Figure 6i, which shows a peak of width ~ 2μm in the correlation of the L4 signal (counting of photons collected into single-mode fiber through lens L4) and the spatially-resolved camera signal obtained through lens L3. The width does roughly agree with estimates of the diffraction-limited performance of the optical system. Note that this includes a diffraction-limited width of ~1μm from the collection into single-mode fibre, a diffraction-limited width of ~1μm from the imaging optics onto the CCD camera, and a ~ 1μm broadening due to the 1μm size of the camera pixels.

Competing Interests: No competing interests were disclosed.

Reviewer Report 01 October 2021

https://doi.org/10.21956/openreseurope.15058.r27548

© **2021 Barredo D.** This is an open access peer review report distributed under the terms of the Creative Commons Attribution License, which permits unrestricted use, distribution, and reproduction in any medium, provided the original work is properly cited.

Daniel Barredo
Laboratoire Charles Fabry, Institut d'Optique Graduate School,CNRS, Université Paris-Saclay, Palaiseau, France

In their manuscript, Bianchet *at al.* report on the characterization of single atom traps using a system of four in-vacuum high NA lenses in a “Maltese cross” geometry. They demonstrate an enhanced light collection efficiency compared to traditional single or dual lens systems, without compromising atom lifetimes, temperatures, or trap sizes.

Maltese cross geometries offer several advantages for single atom manipulation over dual lens optics. Besides a larger solid angle covered by the four lenses, access to the transverse trapping direction allows for an accurate determination of the size of atomic clouds in disordered ensembles, which is otherwise difficult to estimate, and is crucial for the comparison with theoretical models. In patterned arrays, the additional right-angle lenses enable individual addressing of the sites in a 1D lattice, and atom-by-atom assembling to obtain defect free arrays. Furthermore, as mentioned in the manuscript, this geometry has been proposed for novel approaches to engineer strong non-classical correlations between photons in combination with single atoms (e.g. Ref. [31]). From this point of view, the experimental setup described and characterized in the present manuscript is very interesting and timely. This setup and some of the results have been already introduced in Ref. [28], but the current manuscript contains additional

studies about the performance of the traps with single atoms. Overall, the paper is well written and understandable, even for non-specialists. I therefore recommend indexing.

There are a few questions/comments that I would like the authors to consider:

1. I believe replacing the word “measuring” in the title by “detecting” or even “imaging” would be more appropriate.

2. In the section describing the MOT, they state “the horizontally-directed beams are of 0.7mm diameter, whereas the vertical beams are of 2.0mm diameter”. Is this the 1/e^2 size?

3. In the measurement of the atom lifetime in the trap (Fig. 4) and of the single atom temperature (Fig. 5), the survival probability is not zero even for the shortest time interval, but rather 0.9 (they mention 11 % loss probability in the caption of Fig. 5). What is the reason for that? Are these losses related to heating during imaging, for example, or directly associated with the quality of the traps?

4. The authors estimate the trap depth measuring the input power and assuming gaussian optics. This measurement can in principle be done using the atoms as probes, e.g., by spectroscopy to measure induced lightshifts. Have the authors tried this approach?

5. To measure the parametric resonances, the authors pump the atoms in the F=2 manifold and leave the repumper on during the modulation. Do I understand it correctly? If so, why is this necessary?

6. The measured resonances in Fig. 4 are broad. Is it because the modulation is too strong? Have the authors done the experiment with lower modulation depths (< 20 %) to investigate that?

7. Also in Fig. 4, the experimental data are gathered in two different sets at around 12 kHz and 100 kHz. For the low frequency data, they use a modulation time of 30 ms, and for the high frequency range, 150 ms. However, the simulation shows a continuous curve. How is this taken into account in the simulation? I would appreciate more details about the simulation, e.g., if it is a simulation including the three spatial dimensions, or the range of parameters for the Langevin term and the values used.

8. Along the same line, the authors explain that the interpretation of the parametric excitation method is not straightforward for the case of a single atom. Another method usually employed to measure the trapping frequencies (especially the radial one) is to switch the trap off for a few microseconds and on again to excite the radial mode of motion of the atoms in the trap, as it is done, e.g., in Ref [24]. The atoms then oscillate in the trap for a variable time after which one performs a release and recapture experiment. The recapture probability depends on the kinetic energy of the atom and displays oscillations that can be directly mapped onto the trapping frequencies. Possible beatings can then be associated with asymmetries in the trapping potentials. Have the authors explored this method? This can provide additional information to estimate the trap waist.

9. For the 1D lattice the power is reduced from 7 mW to 2.5 mW to “partially compensate the intensity boost implied by the standing wave geometry”. This is still not the expected ratio.

Is this mismatch due to losses at the interfaces of the lenses?

10. In Fig 6i the L1 collection efficiency displays a broad peak which is not symmetric. I would appreciate a few words explaining the origin of this asymmetry.

11. Finally, there is a missing word at the end of page 7. “The power modulation was accomplished by sinusoidally modulating amplitude”. I guess it should read “modulating the amplitude”.

Is the work clearly and accurately presented and does it cite the current literature?
Yes

Is the study design appropriate and does the work have academic merit?
Yes

Are sufficient details of methods and analysis provided to allow replication by others?
Yes

If applicable, is the statistical analysis and its interpretation appropriate?
Yes

Are all the source data underlying the results available to ensure full reproducibility?
Yes

Are the conclusions drawn adequately supported by the results?
Yes

Competing Interests: No competing interests were disclosed.

Reviewer Expertise: cold atoms; optical tweezers; single atoms; Rydberg atoms; quantum simulation; quantum optics

I confirm that I have read this submission and believe that I have an appropriate level of expertise to confirm that it is of an acceptable scientific standard.

Author Response 04 Feb 2022

Lorena C Bianchet

We thank Dr. Barredo for their insightful questions and suggestions. Specific replies are given below:

DB Point 1: I believe replacing the word “measuring” in the title by “detecting” or even “imaging” would be more appropriate.
Reply: As with any scientific article, it is difficult to capture the exact nature of the work in the few words allowed for a title. In our case, the article describes many different operations on the atoms in the trap, including detection and imaging, but also

measurement of the temperature of the atom and atom number statistics, measurement of internal-state dynamics via correlations of resonance fluorescence, the measurement of trap characteristics such as lifetime and trapping beam shape, and manipulations including parametric excitation and lattice confinement. To encompass these many activities, we chose the broad terms “measurement” and “manipulation.” We believe this is an accurate, if not very detailed, title for the work. We also believe that no matter what title we give, the potential reader will have to read the abstract to have a better idea of the content.

DB Point 2: In the section describing the MOT, they state “the horizontally-directed beams are of 0.7mm diameter, whereas the vertical beams are of 2.0mm diameter”. Is this the $1/e^2$ size?
Reply: Yes, it is $1/e^2$. We have added a note in the revised manuscript to clarify this.

DB Point 3: In the measurement of the atom lifetime in the trap (Fig. 4) and of the single atom temperature (Fig. 5), the survival probability is not zero even for the shortest time interval, but rather 0.9 (they mention 11 % loss probability in the caption of Fig. 5). What is the reason for that? Are these losses related to heating during imaging, for example, or directly associated with the quality of the traps?
Reply: One possible explanation for the loss at small delay Δt is expulsion or heating of the atom in the process of turning off and on the MOT beams. This could arise if, for example, the intensity balance of the six MOT beams is not maintained during turn-off and turn-on.

DB Point 4: The authors estimate the trap depth measuring the input power and assuming gaussian optics. This measurement can in principle be done using the atoms as probes, e.g., by spectroscopy to measure induced lightshifts. Have the authors tried this approach?
Reply: Yes, in fact, we have performed a spectroscopy measurement in order to have a more accurate measurement of the trap depth. The results are in agreement with the estimates made in this article. A proper description of the technique is a bit too involved to include in this article, and is being prepared for publication elsewhere.

DB Point 5: To measure the parametric resonances, the authors pump the atoms in the F=2 manifold and leave the repumper on during the modulation. Do I understand it correctly? If so, why is this necessary?
Reply: Yes, the repumper was left on in this experiment. With the repumper on, and no cooler light present, the atom will be quickly pumped into the F=2 ground state and remain in that state. The atom’s internal state is not important to the parametric excitation process, because the light shifts are nearly identical for all ground states. Consequently, the repumper or its absence should have no important effect on the parametric excitation by the FORT light. At the same time, our simulations are only able to reproduce the data if there is a significant heating of the atom during the parametric excitation process, beyond what is expected from scattering of the FORT light. The repumper could potentially contribute to this heating, through off-resonance scattering, or scattering of laser sidebands near the F=2 → F’ resonances.

DB Point 6: The measured resonances in Fig. 4 are broad. Is it because the modulation is too strong? Have the authors done the experiment with lower modulation depths (< 20 %) to investigate that?
Reply: Yes, we did measure with lower modulation depths. With 1% of modulation depth,

the resonance was difficult to see. Between 6% and 20%, we did not observe that the width of the resonance changed significantly. For this reason, we do not believe that the principal reason for the resonance widths is power broadening. Rather, we believe it is a consequence of the anharmonicity of the FORT potential.

DB Point 7: Also in Fig. 4, the experimental data are gathered in two different sets at around 12 kHz and 100 kHz. For the low frequency data, they use a modulation time of 30 ms, and for the high frequency range, 150 ms. However, the simulation shows a continuous curve. How is this taken into account in the simulation? I would appreciate more details about the simulation, e.g., if it is a simulation including the three spatial dimensions, or the range of parameters for the Langevin term and the values used.
Reply: We thank Dr. Barredo especially for this question, which made us aware of a mistake in the article. Both the experiment and simulations used a modulation time of 150 ms for frequencies $\leq$ 30 kHz, and of 30 ms for larger frequencies. These times were reversed in version 1, and have been corrected in version 2. In Figure 4, a statistically significant step is in fact visible from 30 kHz to 31 kHz. The simulation is indeed in three spatial dimensions. The Langevin term, described in the article as "heating rate of 2.5 recoil/ms (6.5 recoil/ms) [for $\leq$ 30 kHz (> 30 kHz)]" is implemented as an isotropic diffusion in momentum space. The exact calculation method, implemented in Julia, is included in the repository at https://doi.org/10.5281/zenodo.5118863.

DB Point 8: Along the same line, the authors explain that the interpretation of the parametric excitation method is not straightforward for the case of a single atom. Another method usually employed to measure the trapping frequencies (especially the radial one) is to switch the trap off for a few microseconds and on again to excite the radial mode of motion of the atoms in the trap, as it is done, e.g., in Ref [24]. The atoms then oscillate in the trap for a variable time after which one performs a release and recapture experiment. The recapture probability depends on the kinetic energy of the atom and displays oscillations that can be directly mapped onto the trapping frequencies. Possible beatings can then be associated with asymmetries in the trapping potentials. Have the authors explored this method? This can provide additional information to estimate the trap waist.
Reply: We have not used this method.

DB Point 9: For the 1D lattice the power is reduced from 7 mW to 2.5 mW to "partially compensate the intensity boost implied by the standing wave geometry". This is still not the expected ratio. Is this mismatch due to losses at the interfaces of the lenses?
Reply: We estimate the additional optical losses for the retro-reflected beam, i.e., losses incurred in going from the FORT focus to the mirror and back again, to be about 14% (or 1 mW of 7 mW) . This loss is expected to be about equally divided between losses from reflection at lens surfaces and reflection at vacuum window surfaces. In the absence of these losses, retro-reflection (at the same input power) would produce a factor of 4 increase in intensity at the antinodes. With 14% losses, retro-reflection at the same input power would produce a factor of 3.7 increase in intensity. An equal-intensity compensation would thus require 1.9 mW with losses, or 1.75 mW without. By reducing to 2.5 mW, we are thus operating with slightly deeper traps in the lattice case than in the single-pass case.

DB Point 10: In Fig 6i the L1 collection efficiency displays a broad peak which is not symmetric. I

would appreciate a few words explaining the origin of this asymmetry.
Reply: We have added a note in the revised manuscript to clarify this.

DB Point 11: Finally, there is a missing word at the end of page 7. "The power modulation was accomplished by sinusoidally modulating amplitude". I guess it should read "modulating the amplitude".
Reply: We have fixed this in the revision.

Competing Interests: No competing interests were disclosed.